RSC Advances

ROYAL SOCIETY OF CHEMISTRY

www.rsc.org/advances

RSC Advances

Real-time monitoring of self-assembling wormlike micelle formation by organic transistors

V. Preziosi[a*]**, G. Tarabella**[b*]**, P. D'Angelo**[b]**, A. Romeo**[b]**, M. Barra**[a]**, S. Guido**[c]**, A. Cassinese**[a]**, S. Iannotta**[b]

Thanks to their appealing rheological properties, nowadays micellar solutions play a fundamental role in many industrial sectors, including personal care products, cosmetics and pharmaceuticals. The use of these solutions and their effectiveness in the desired application is, however, strongly dependent on the
10 specific micellar aggregation form and the related degree of entanglement. To this end, it should be mentioned that, still today, the type and size of the micellar aggregates in a solution can be investigated only by using sophisticated laboratory techniques which are very difficult to be applied directly in real industrial production sites. In this paper, we demonstrate that organic electrochemical transistors (OECTs) based on PEDOT:PSS active channels can be used to reveal the presence of worm-like micelles
15 in surfactant-salt aqueous solutions. In the worm-like regime the response of these devices displays distinctive features in comparison with those exhibited when pure surfactant solutions, containing only spherical micelles, are analysed. Our results could pave the way to the development of a new class of portable and user-friendly devices, suitable for the in-situ monitoring of morphological transitions involving micellar aggregates.

20 Introduction

Nowadays, surfactants play an extraordinary role in the worldwide industry due to their almost ubiquitous applications in the finalization of products such as detergents, cosmetics, pharmaceuticals, foods, etc., as witnessed by the current global
25 production of surfactants largely exceeding 10 Mton per year[1]. The importance of surfactants is related to the amphiphilic character of their structure, determined by the contemporary presence of hydrophilic (water-soluble) and hydrophobic (water-insoluble) groups. In this way, surfactants are able to promote the
30 miscibility of otherwise immiscible liquids (e.g. water and oil) by decreasing the interfacial tension between them[2]. This process favours the stabilization of emulsions and foams and makes them suitable for use in consumer goods. Another distinctive feature of surfactants is their ability, when dispersed in an aqueous solution
35 and above a certain critical concentration value (CMC), to aggregate forming micelles of various shape and size. This self-assembling process is basically driven by the surfactant requirement to reach a stable energy condition, obtained by means of a structural rearrangement that minimizes the exposure
40 of the hydrophobic tails to water.

In the last years, the micellization phenomenon in surfactant systems has been widely studied, analysing the specific influence of several factors (e.g., the surfactant concentration, the solvent type, the solution temperature and the addition of other
45 substances), on micelles formation and their final shape[3-7]. In particular, it was demonstrated that the addition of organic or inorganic salts to surfactant aqueous solutions promotes the conversion of basic spherical micelles (i.e. the simplest micellar aggregation form) in more complex structures exhibiting worm-
50 like shape[8] with a variable degree of entanglement[4, 9]. Nowadays, worm-like micellar solutions are widely studied for their peculiar rheological properties[7-11,12-13], which make them increasingly attractive in many industrial processes such as in enhanced oil recovery, where they are used as fracturing fluids, or in cosmetics
55 and biomedical industries[14, 15].

As widely reported in literature, in the worm-like systems the counterion nature of the added salt can induce strong structural changes, in terms of micellar flexibility, characteristic lengths and scission energy (that is the energy required to create two end-
60 caps from a semi-infinite cylinder), according to whether or not it penetrates into the micelle creating a strong binding[7,16]. However, small changes in worm-like micelles formulation can also drastically affect their structure and dynamics, resulting in a different macroscopic rheological response. As worm-like
65 micelles show many analogies with polymers, they are also called "living polymers"[17,18] and they can be used as model fluids to investigate about polymers behavior[9]. Nevertheless, unlike polymers, worm-like micelles can rather easily break and

reversibly return to their spherical structure. Thus, from a theoretical point of view, worm-like micelles can be described by a model based on the reptation theory[18], which describes the rheological properties of entangled polymeric chains, but including the effects of reversible scission kinetics, derived by Cates[9] and still widely used[19,20]. Such model basically states that micelles relax mono-exponentially with a single characteristic time τ_R, that takes into account both reptation and breaking processes. In this situation their linear viscoelastic properties, represented by G' and G'' spectra, can be accurately described by the Maxwell-fluid model with a single relaxation time. In this model, it should be remembered that *G'* is defined as the *elastic* (or *storage) modulus*, which takes into account the stored energy, while *G'' is defined as* the *viscous* (or *loss*) *modulus,* which is, instead, a measure of the mechanically energy dissipated in the material. According to the Maxwell-fluid model, G' and G'' can be described by the following equations:

$$G'(\omega) = \frac{\omega^2 \tau_R^2}{1+\omega^2 \tau_R^2} G_0 \qquad \text{eq. 1)}$$

$$G''(\omega) = \frac{\omega \tau_R}{1+\omega^2 \tau_R^2} G_0 \qquad \text{eq. 2)}$$

where ω is the frequency, τ_R is the relaxation time and is approximately the inverse of the crossover frequency between G' and G'', and G_0 is the plateau modulus, that is the high frequency storage modulus. A typical Maxwellian behavior, expressed by eq 1) and 2), can be also described by a perfect semi-circle in the so-called Cole-Cole plot, where G'' is plotted as a function of G'.

From literature it is also known that when a steady shear is applied to a worm-like structure, the solution undergoes a transition between a homogenous and a non-homogeneous shear flow, the latter being characterized by the formation of macroscopic regions in the fluid with different viscosity (shear banding[20-22]. Shear banding is an abrupt transition that occurs at a critical shear rate, $\dot{\gamma}^*$, in correspondence to which the flow curve exhibits a discontinuity of slope (τ_p), followed by a stress plateau that stretches over more than a decade in shear rates. At higher shear rates, a further increase of the stress takes place. However, in some worm-like systems the plateau is not totally flat but exhibits a slight increase as a function of the shear rate.

Despite the enormous scientific interest for the rheological properties of worm-like systems and for the related practical applications, it has to be pointed out that, still today, the presence of worm-like aggregates in a surfactant aqueous solution is checked by specific laboratory techniques displaying different levels of complexity and accuracy. Among these, Laser Light Scattering (LLS), Rheometry, Cryogenic-Transmission-Electron Microscopy (Cryo-TEM) and Small Angle Neutron Scattering (SANS) are some of the most used experimental approaches[4, 8, 23-26].

Recently, it was reported the possibility to use an organic electrochemical transistor (OECT) based on a PEDOT:PSS (poly(3,4-ethylenedioxythiophene) doped with poly(styrene sulfonate)) channel as a portable device to monitor the formation of micellar aggregates in a surfactant (namely, cetyltrimethylammonium bromide - CTAB) solution[27] and for liposome sensing[28]. In an OECT, the PEDOT:PSS channel connects two electrodes (source and drain) and is in contact with an electrolytic medium, that acts as the gate dielectric. The device is completed by a third electrode (gate) which is directly immersed in the electrolyte solution. When a positive voltage (V_{GS}) is applied between the gate and source, the positively charged species contained in the electrolyte are pushed away from the gate electrode and are injected into the PEDOT:PSS backbone, neutralizing the PSS- sites and de-doping the active channel[29,30]. Hence, this process provides a reversible V_{GS}-controlled decrease of the drain-source current (I_{DS}) which can flow along the active channel for a given drain-source voltage (V_{DS}). More in detail, it was shown that, if the CTAB solution is employed as electrolyte for the OECT gating, the related current modulation rapidly increases when the surfactant concentration overcomes the CMC value[27]. By means of a detailed UV/VIS optical analysis, this phenomenon was found to be directly related to the better capability of CTA+ micelles with respect to metallic cations, for instance, to reversibly de-dope the PEDOT:PSS channel by electrically balancing the PSS- sites.

Inspired by this initial work, here we investigate the response of OECTs based on PEDOT:PSS in presence of more complex micellar aggregates characterized by an elongated worm-like shape. To this purpose, two different CTAB systems, prepared through the addition of both organic (sodium salycilate - NaSal) and inorganic (Potassium Bromide - KBr) salts, have been employed. First, the rheological properties of the selected solutions have been studied to confirm the formation of the worm-like aggregation. Then, the OECT electrical responses in presence of worm-like solutions have been evaluated by means of both steady state and dynamic electrical measurements, and have been compared with those achievable in pure NaSal, KBr and CTAB solutions. Our results demonstrate that the OECT behaviour is strongly affected by the size of the micellar aggregates and the related level of entanglement. This last feature, in particular, seems to be a major factor in defining the way in which micelles can electrically interact with the PEDOT:PSS chains.

Materials and methods

A PEDOT:PSS aqueous dispersion (Clevios PH500) was purchased from Heraeus Conductive Polymers Division. In order to get films with enhanced conductivity (up to 10^2 S/cm), the commercial PEDOT:PSS dispersion was doped with ethylene glycol (Sigma Aldrich, 20% in vol.) and dodecyl-benzene sulfonic acid (DBSA) surfactant (Sigma Aldrich, 0.05% in vol.). The final solution was spun on glass slides, partially covered with Kapton tape in order to define the device active channel. Films were spin-coated with a first ramp of 6 sec at 450 rpm with acceleration up to 1500 rpm, followed by a plateau of 30 sec at 1500 rpm (final measured thickness of ~80 nm), and then were baked in air on a hotplate, at 120 °C, for 1 hour. After the annealing process, the Kapton tape was removed resulting in a 2 cm long, 1 mm wide PEDOT:PSS channel. For all devices considered in this work, a poly(dimethylsiloxane) (PDMS) well was attached on the active channel to confine the electrolyte solution. In all cases, a Gold (Au) wire immersed in the solution was used as the gate electrode. Fig. 1 reports schematically the

complete layout of the investigated devices. The OECT electrical responses were tested with two different measurement stations, both using 2-channel source-meters (Agilent B2902A and Keithley 2612A).
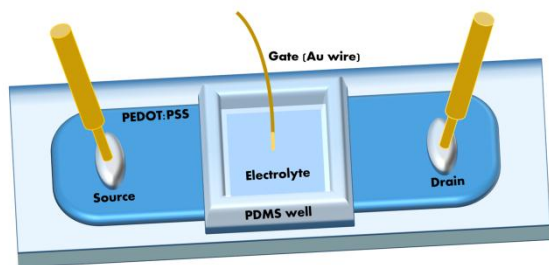

5
Fig. 1 Schematic layout of our OECT device. The active area is defined by the overlapping region between the PDMS well (electrolyte reservoir) and the PEDOT:PSS channel. A gold wire immersed into the electrolyte acts as the gate electrode.

10
As electrolytes, the aqueous solutions reported in the following table (Table 1) have been considered: where CTAB ($C_{19}H_{42}BrN$, PM=364.5, purity $\geq$ 98%) and NaSal (HOC_6H_4COONa, PM= 160.10, purity $\geq$ 98%) were purchased from Sigma Aldrich, while 15 KBr (PM=119.00) was purchased by VWR International Ltd.

Table 1 Electrolytic solutions analysed in this work with concentration and conductivity values

	Electrolyte	**C [M]**	**Conductivity [mS/cm]**
1	CTAB	0.01	0.29
2	NaSal	0.045	0.72
3	CTAB	0.05	0.37
4	KBr	0.25	28.75
5	KBr	0.5	52.00
6	CTAB + KBr	0.01 - 0.25	41.00
7	CTAB + KBr	0.01 - 0.5	55.00
8	CTAB +NaSal	0.05 - 0.045	4.74

20
The solutions were prepared in ambient conditions and their conductivity was estimated by a conductivity meter (PC 2700, Eutech Instruments) at ~25 °C. Before their use as electrolytes, the worm-like micellar solutions were left to completely stabilize 25 for an adequate amount of time (2 days). Prior to every OECT measurement, micellar solutions were stirred for 30 min.
Rheological measurements were performed using a controlled-stress rheometer (Bohlin Instruments CVO 120) operating both in continuous shear and in dynamic oscillatory mode using a 60 30 mm, 1 deg smooth stainless steel cone-plate geometry. The sample was loaded on the plate center and possible air bubbles were removed. All measurements were performed at room temperature (~23 °C).

35

Results and discussion

Rheological characterization

CTAB has been widely used in literature as surfactant for its ability to form micellar structures of different shape at 40 concentrations higher than its critical micellar concentration (CMC ~ 10^{-3} M at 298K). It has also been reported that the addition of a salt to a CTAB solution can largely shift the CMC value, thus favoring the formation of worm-like micelles[7].
Moreover, the structure and dynamics of worm-like micelles are 45 highly modified by the specific nature of the salt counterion, which affects directly the macroscopic rheological behaviour of the final solutions[31-37]. In the CTAB/Salt systems, in particular, it has been widely demonstrated that the interaction mechanism of Sal$^-$ ions is different to that of Br$^-$ ions on the surfactant 50 structure[38-39]. Indeed, while the former can deeply penetrate the micellar structure (the aromatic part of the counterion is solubilized in the micelle, increasing the degree of binding), the latter are non-penetrating counterions providing a weak interaction with the surfactant and a consequent different 55 rheological response[8].
In order to experimentally assess the rheological features of the worm-like systems (CTAB+KBr and CTAB+NaSaL) investigated in this work, their viscoelastic behaviour was evaluated by applying oscillatory deformations to the samples 60 and measuring the corresponding G' and G'' spectra. In Fig. 2A, G' and G'' are plotted as a function of the angular frequency in the range 0.2 - 20 rad/s for the CTAB+KBr solution. For this system, the viscous modulus G'' predominates over the elastic modulus G' throughout almost the whole frequency range. 65 Moreover, especially in the low frequency range, the low elasticity of this system results in G' values close to the instrument sensitivity. Fig. S1A (see Supporting Information) represents the continuous shear test (viscosity *vs* shear rate) performed on this sample confirming the non-Newtonian 70 character of this worm-like fluid and, in particular, the occurrence of a shear thinning behaviour with the viscosity decreasing as a function of the shear rate[40]. In fig.2B, the linear viscoelastic response of the CTAB+NaSal system is shown. Here, G' and G'' are measured in the frequency range 0.01 - 10 rad/s, and both 75 moduli values are at least two orders of magnitude higher than those of the CTAB+KBr system. The viscosity measurement reported in fig.S1B for this system reveals a Newtonian behaviour featuring a constant viscosity up to about 0.3 s^{-1} and a decreasing trend occurring for higher shear rates. The calculated 80 slope of the power law is about 0.85, which is in agreement with a semi-dilute polymer behaviour[41]. In fig. 2C, a Cole-Cole representation for the CTAB+NaSal system, where G'' is plotted as a function of G', is presented. As shown, the experimental data (symbols) can be very well fitted by a semi-circle equation (solid 85 line) corresponding to an ideal Maxwell element with a single relaxation time (τ_R =1.6 s).
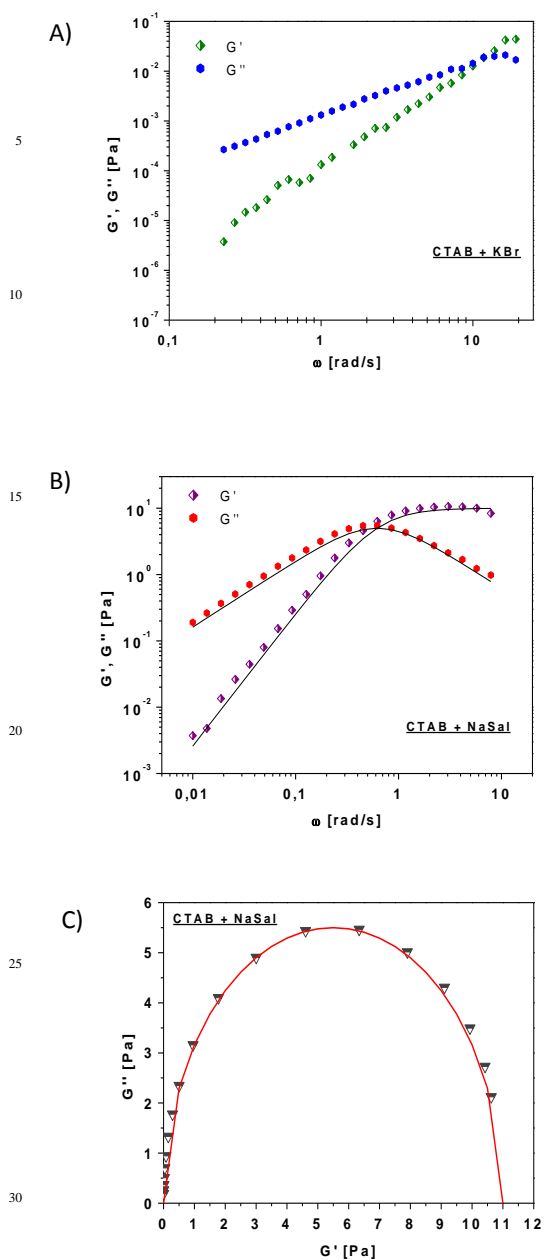
90

A)

B)

C)

Fig. 2 Elastic (G') ad viscous (G'') modulus as a function of the oscillation frequency measured for A) CTAB+KBr and B) CTAB+NaSal worm-like solutions. Solid lines in panel B are the fits calculated from Eq. 1 and 2. C) Cole-Cole plot for CTAB+NaSal system (the dashed red line corresponds to the fit with the equation of a semi-circle).

In Fig.3, the shear stress as a function of the shear rate for the two investigated systems is also displayed. In Fig. 3A (CTAB+KBr), an increasing trend of the shear stress, τ, against the shear rate, $\dot{\gamma}$, is shown, while for CTAB+NaSal (Fig. 3B) three regions are visible; the first one corresponds to a Newtonian regime, where the stress varies linearly with the shear rate; in the second one, the shear stress increases up to at a value of the shear rate, $\dot{\gamma}^*$=0.5 s^{-1}, where the flow curve exhibits a discontinuity of slope, followed by a stress plateau for two decades in $\dot{\gamma}$; in the third one, an increase at higher shear rates ($\dot{\gamma}$ ~20 s^{-1}) occurs.
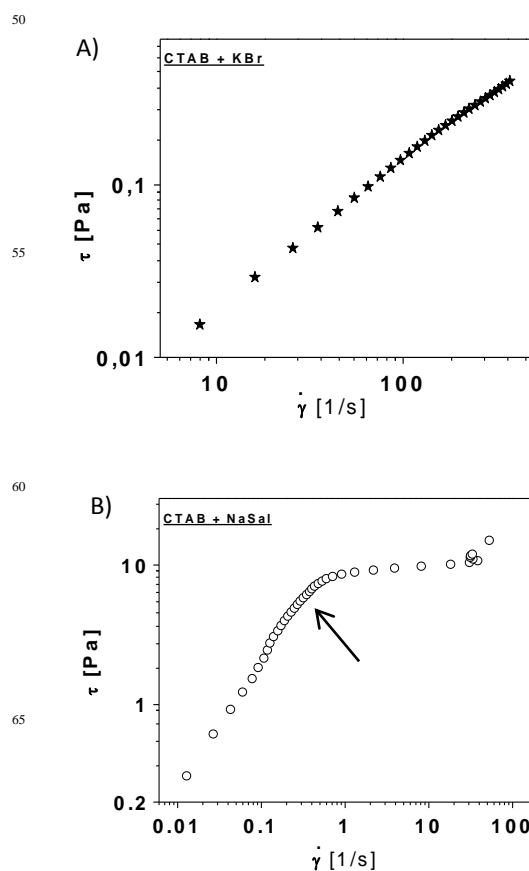
A)

B)

Fig. 3 Steady state viscosity response for A) CTAB+KBr micellar structure and B) CTAB+NaSal. In panel B) the onset (indicated by the arrow) of the stress plateau is at the critical shear rate $\dot{\gamma}^*$ = 0.5 s^{-1}.

All the above discussed rheological data make clear that worm-like micellar structures are present in both the two CTAB-based systems here analyzed. The micelles, however, are characterized by a different size and level of entanglement in close agreement with the data reported in the literature[9].

Basically, the CTAB+KBr systems display a poor viscoelastic response with the related worm-like micelles being scarcely entangled. Laser Light Scattering (LLS) measurements have revealed that, in the CTAB+KBr solutions having a CTAB concentration equal to 0.01 M, the hydrodinamic correlation length (R_h) of the worm-like micelles increases from 20 nm up to about 40 nm when the KBr concentration goes from 0.2 to 0.6M [38]. Moreover, other experiments suggest that, in this system, the persistence length, l_p of the micelles (defined as the maximum length of the uninterrupted polymer chain persisting in a particular direction) is about 15 nm,[9, 25,38]

The situation is quite different for the CTAB+NaSal solution which, as previously observed, exhibits an enhanced viscoelastic behavior. According to the literature data, for a CTAB + NaSal solution with CTAB=0.05M and NaSal=0.05M, the hydrodynamic size R_h is found to be about 10 nm[36], whereas l_p is

instead of the order of 40 nm [18,20,39]. It can be thus concluded that, in presence of the NaSal, which is able to penetrate the initial CTAB micellar structures, the final micelles assume a cylindrical shape having an increased aspect ratio (i.e. long and thin micelles), This feature strongly supports the formation of entangled structures which make this fluid more similar to a gel-like system.

OECT electrical response

For the OECT characterization, the use of a Gold wire as the gate electrode (see Fig.1) for all the considered solutions allowed working in a purely capacitive mode, without the occurrence of any Faradaic reaction at the gate/electrolyte interface[42]. Platinum was not taken into consideration as gate material to avoid (as verified in some preliminary tests) the oxidation reaction involving the -OH group in the Salicylate anion (SaL^-), similarly to what observed for the OECT operation in an aqueous suspension of a synthetic eumelanin[43].

OECT modulation ratio

In a first set of experiments, the OECT response characterization was carried out by recording the drain-source current (I_{DS}) and the corresponding gate-source current (I_{GS}) as a function of time, while the drain-source (V_{DS}) voltage was set constant at -0.4V and the gate-source voltage (V_{GS}) was pulsed from 0 to 0.6V with a step (ΔV_{GS}) of 0.1V (transient current measurements). The duration of both $V_{GS} > 0V$ and $V_{GS} = 0V$ steps was set at 60 s, in order to allow the I_{DS} current reaching a nearly steady state and to recover the initial ON current value (I_0), respectively[27]. According to our experimental results, for the complex electrolytic media considered in this work, the application of V_{GS} voltages not exceeding 0.6 V remarkably improves the device testing reproducibility.

Fig. 4A reports a typical I_{DS} vs time curve recorded for a CTAB+KBr worm-like solution covering the OECT active channel. In the same plot, the I_{GS} measurement is also shown. These curves clearly indicate that the OECT can work properly also in the complex surfactant-salt mixed solutions here investigated. Indeed, in agreement with the aforementioned OECT working principle, when a $V_{GS} > 0$ pulse is applied, the I_{DS} current decreases significantly, while the I_{GS} remains orders of magnitude lower than I_{DS}, neglecting the presence of the displacement current spikes which correspond to the V_{GS} changes and are related to the capacitive coupling between the gate electrode and the electrolyte[29].

To compare the OECT performances in the different solutions, the current modulation ratio, defined as $\Delta I/I_0 = |[I(V_{GS}>0) - I(V_{GS}=0)]/I(V_{GS}=0)|$[44], was extracted from the transient current measurements as a function of V_{GS}. Fig.4B and 4C summarize the results achieved for the two different systems (CTAB+KBr and CTAB+NaSaL), respectively, investigated in this work. In the case of CTAB+KBr, it is possible to observe that the OECT current modulation is significantly enhanced by the presence of worm-like micellar aggregates (CTAB+KBr solutions), in comparison with those recorded with the pure KBr (0.5M) salt or when the solution with only spherical micelles (CTAB 0.01M) is considered. In particular, these data demonstrate that the OECT sensitivity in the worm-like regime is higher in the whole V_{GS}

range here investigated. Fig.4B shows also that, when the KBr concentration is increased (from 0.25M to 0.5M), the OECT current modulation undergoes a further enhancement. This feature cannot be simply ascribed to the increased presence of the salt, since (see the corresponding curves in fig.S3A) the OECT modulation response in pure KBr aqueous solutions is the same for these two KBr concentrations. Consequently, this finding is rather related to the shift of the average size of the worm-like aggregates which hydrodinamic correlation length (R_h) is almost doubled for C_{KB} going from 0.25M to 0.5M[38]. The analysis of the OECT response for the CTAB+NaSaL system (Fig.4C) provides a very different scenario. In this case, indeed, it can be easily observed that the OECT current modulation ($\Delta I/I_0$) in presence of the spherical micelles (CTAB 0.05M) is the highest, in comparison, in particular, to what occurs with the worm-like aggregates obtained by mixing CTAB and NaSal.
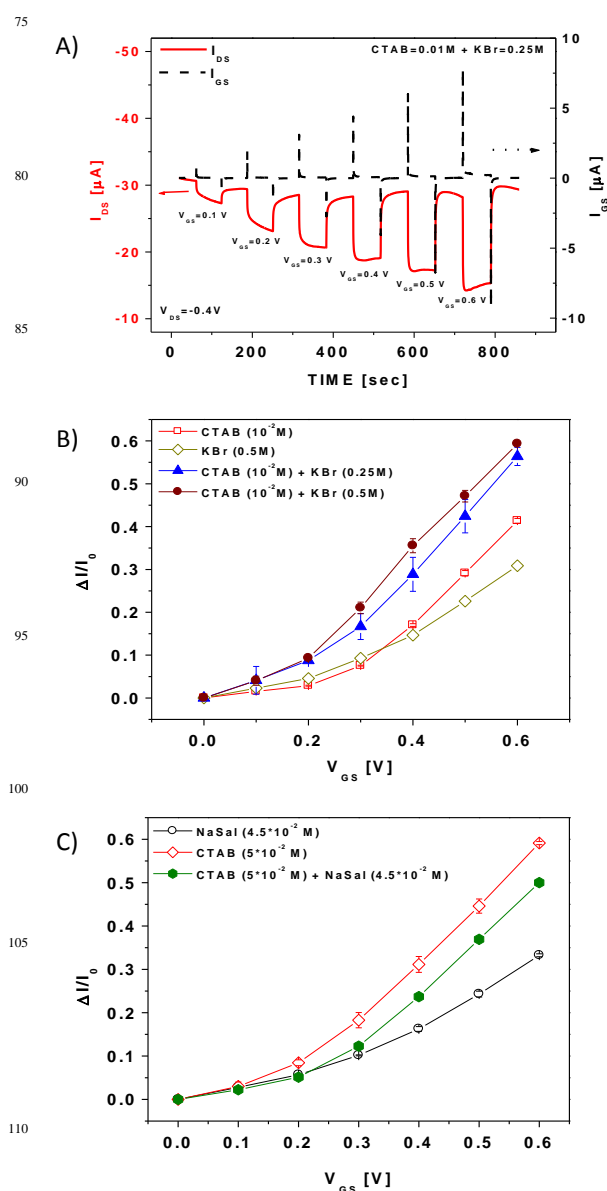
Fig. 4 A) I_{DS} (left axis) and I_{GATE} (right axis) currents recorded as a function of time with V_{GS} pulsed from 0 to 0.6V and V_{DS} set at -0.4V for an OECT with a CTAB+KBr solution used as electrolyte. The OECT modulation response ($\Delta I=(I-I_0)/I_0$) vs V_{GS} extracted for B) (CTAB, KBr and CTAB+KBr) and C) (CTAB, NaSal and CTAB+NaSal) solutions. In these plots, worm-like solutions are identified by closed symbols. ΔI values are extracted as average of at least 3 measurements. The error bars represent the standard deviations.

Very significantly, this last result reveals that, for this system, the level of entanglement of the micellar structures rather than the simple presence of the worm-like micelles is able to dominate the OECT current modulation behaviour.

FET-Like Transfers and real-time measurements

To get a further confirmation of the experimental results discussed above, a complementary OECT measurement was performed by recording directly the transfer-curves of the transistor (Fig.5). Here, V_{GS} was varied between 0 and 0.6 V with step of 0.1V and, differently from the transient I_{DS} measurements, the time interval between the V_{GS} application and the I_{DS} value recording was set at 5 sec while V_{GS} was continuously raised up from 0V to 0.6V without the restoring step at V_{GS}=0V. Transfer curves gave a further indication about the selectivity of the OECT response according to the specific morphology of the investigated micellar aggregates. In particular, it was observed that those solutions, providing enhanced OECT current modulations (as reported in Figs. 4B and 4C), also tend to shift the transfer curves to lower gate voltages with an equivalent decrease of the ON current (I_{DS} at V_{GS}=0V)[45]. Interestingly, current modulation data extracted from transfer-curves (see Fig.S2) exhibit an almost perfect agreement with results in Fig.4. So, while the CTAB+KBr worm-like solutions are shown to provide the OECT with an increased modulation capability if compared with the parent CTAB (0.01M) solution containing only spherical micelles, the entangled worm-like micelles in the CTAB+NaSaL system are confirmed to be less effective in de-doping the PEDOT:PSS active channel.
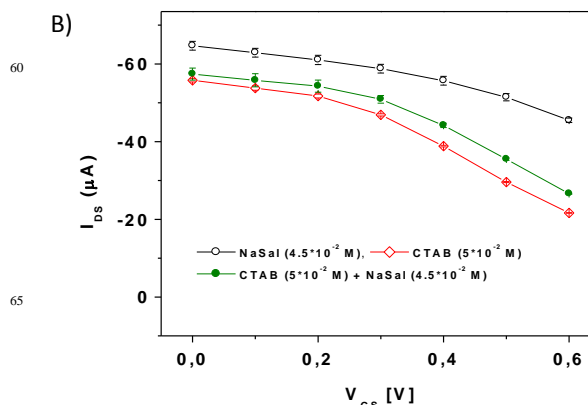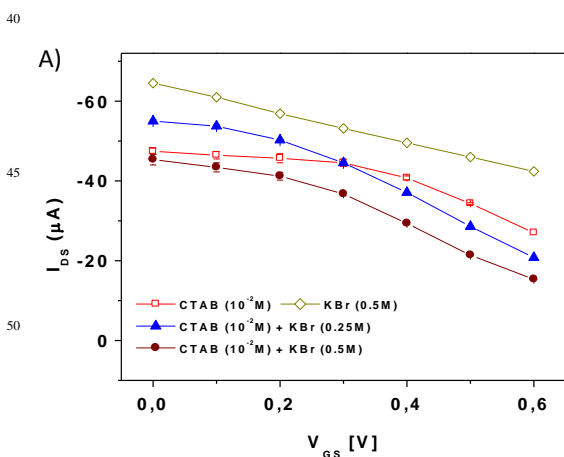

Fig. 5 OECT transfer-curves measured as a function of gate voltage (V_{GS}) and with V_{DS}=-0.4V for A) (CTAB, KBr and CTAB+KBr) and B) (CTAB, NaSal and CTAB+NaSal) solutions. In these plots, worm-like solutions are identified by closed symbols

Finally, in order to demonstrate with more evidence the possibility to use OECTs for monitoring the *real-time* formation of micelles, we performed a set of flow measurements. For both micellar solutions investigated here (CTAB+KBr and CTAB+NaSal), the I_{DS} current was recorded upon progressive and real-time substitution of the electrolyte in the PDMS well in the following order: CTAB 0.01M → CTAB 0.01M+KBr 0.25M → CTAB 0.01M +KBr 0.5M, and CTAB 0.05M → CTAB 0.05M +NaSal 0.045M, respectively. These measurements provide a direct and intuitive dynamic picture of the changes taking place in complex systems, witnessing the general ability of electrochemical devices in displaying real-time variations that can be induced in rheological systems of interest. The two surfactant-salt systems were analysed separately as shown in Fig.6. V_{GS} was swept during the different phases of the experiment between the values +0.4 V and -0.4 V, as reported explicitly in the Fig.6. V_{DS}, instead, was set again at -0.4V. It should be mentioned that, in this case, the application of negative gate-steps allowed inducing a fast recovery of the original value of the I_{DS} current, corresponding to the ON state (V_{GS}=0V) of the device. In this respect, indeed, the recovery of the channel current induced by the depletion of micelles in the polymer channel is field-assisted (application of negative V_{GS}), unlike the case of current modulation (depletion assisted by a diffusive mechanism), and FET-like transfer characteristic measurements (where the step-like increase of V_{GS} corresponds to a progressive injection of micelles into the polymer).

In any case, in full agreement with the previously discussed data, the real-time flow measurements confirm once again the different behavior of the two worm-like micellar aggregates with respect to the corresponding spherical micelles.
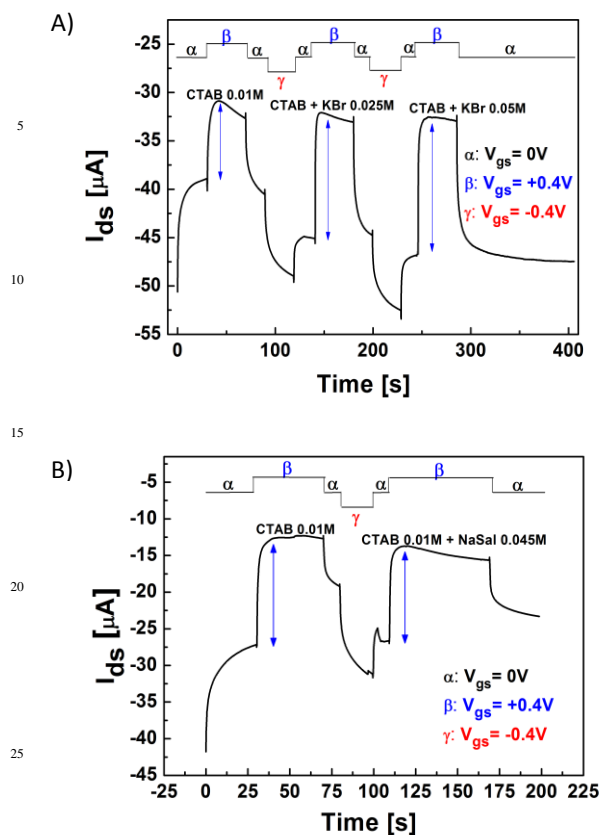
A)

B)

Fig. 6 Real time flow measurements: I_{DS} vs time curves recorded in an OECT after the sequential in-situ injection of the different solutions for
30 A) (CTAB+KBr) and B) (CTAB+NaSal) systems. Insets show the various gate voltages applied within each step while V_{DS} was kept fixed at -0.4V.

The main aspect emerging from these real-time measurements regards the reliability of all the measurements carried out so far. In fact, the self-consistent trends, showed both by the current
35 modulation curves and transfer characteristics recorded in presence of different micellar aggregates, are the result of reversible interactions between the conducting channel and the electrolytes analysed. Therefore, irreversible changes involving the polymer conducting state, such as those induced by repeated
40 measurements in presence of other complex electrolytes, can be ruled out in these experiments.

Discussion and conclusions

In this work, we have tested the electrical response of OECTs
45 based on PEDOT:PSS active channels when surfactant-salt aqueous solutions containing worm-like micelles are employed as electrolytic media. First of all, our results demonstrate that OECTs are able to work properly and reliably also in presence of these complex liquids.
50 More specifically, it was found that, in comparison with a CTAB solution having the same surfactant concentration, CTAB+KBr worm-like micelles provide an enhanced current modulation and the related transfer-curves tend to shifted towards lower V_{GS} voltages. The opposite trends were observed for the
55 CTAB+NaSaL gel-like system, whose entangled worm-like

micelles result to be less effective in de-doping the PEDOT:PSS channel.

It is quite important to highlight, once again, that these differences in the OECT behaviour are not trivially related to the
60 different types or concentrations of the salts contained in the solutions. Despite the salt concentration affects basically the final solution conductivity (which, see TABLE 1, in the worm-like solutions is always higher than the corresponding spherical micellar regime), fig.S3A demonstrates unambiguously that the
65 OECT modulation ratio is practically the same for all the types and concentrations of salts considered in this work. In particular, in these pure salt aqueous solutions, ΔI remains about 0.3 even for V_{GS}=0.6V.

Even more importantly, the changes in the OECT response
70 detected for the previously analyzed CTAB+KBr and CTAB+NaSal solutions cannot be ascribed to the difference in the CTAB concentration (0.01 M vs 0.05M, respectively). In this regard, we performed a further experiment investigating the OECT response in a worm-like solution having CTAB 0.05M +
75 KBr 0.5M. In fig. S3B, the corresponding current modulation ratio is compared with that achieved for the pure CTAB 0.05M solution (with spherical micelles) and with the gel-like CTAB 0.05 M + NaSal 0.045 M fluid. This comparison makes definitely clear that, though keeping fixed the surfactant concentration
80 (CTAB 0.05M), the OECT response is remarkably depending on the size of the micellar structures and, notably, on their level of entanglement.

As a whole, our experimental observations seem to depict a scenario where the ability of the cationic species contained in the
85 solutions to penetrate into the porous PEDOT:PSS film plays the fundamental role in determining the final OECT modulation response. In this framework, consequently, the level of entanglement of the micellar structures can strongly limit their effectiveness to interact and electrically balance the PSS⁻ sites
90 thus providing a reduced de-doping effect of the transistor active channel (i.e. lower ΔI).

In conclusions, the results discussed in this work confirm the relevance of PEDOT:PSS OECTs to be applied as portable and miniaturized electronic devices operating in complex surfactant
95 solutions, for monitoring the presence and the in-situ formation of micellar aggregates having different shape and size. Future work will be devoted to analyze the OECT behaviour when in contact with micellar solutions based on various surfactants exhibiting different CMC values and progressively increasing size of the
100 starting spherical micelles.

Notes and references

ᵃ CNR-SPIN and Physics Dep., University Federico II, Piaz. Tecchio 80, I-80125 Naples, Italy. Email: valentina.preziosi@unina.it

5 *ᵇ IMEM-CNR, Parco Area delle Scienze 37/A, I-43124 Parma, Italy. Email: giuseppe.tarabella@imem.cnr.it*

ᶜ Department of Chemical, Materials and Production Engineering - University Federico II - Piaz. Tecchio 80, I-80125 Naples, Italy

10

1   D. Myers, *Surfactant science and technology*, John Wiley & Sons, 2005.

2   V. B. Fainerman, N. Mucic, V. Pradines, E. V. Aksenenko and R. Miller, *Langmuir*, 2013, **29**, 13783-13789.

15 3   Z. Chu, C. A. Dreiss and Y. Feng, *Chemical Society Reviews*, 2013, **42**, 7174-7203.

4   R. D. Koehler, S. R. Raghavan and E. W. Kaler, *The Journal of Physical Chemistry B*, 2000, **104**, 11035-11044.

5   Z. Lin, J. Cai, L. Scriven and H. Davis, *The Journal of Physical Chemistry*, 1994, **98**, 5984-5993.

20 6   Z. Lin, *Langmuir*, 1996, **12**, 1729-1737.

7   C. Oelschlaeger, P. Suwita and N. Willenbacher, *Langmuir*, 2010, **26**, 7045-7053.

8   C. A. Dreiss, *Soft Matter*, 2007, **3**, 956-970.

25 9   M. Cates and S. Candau, *Journal of Physics: Condensed Matter*, 1990, **2**, 6869-6892.

10 B. Lin, S. Mohanty, A. V. McCormick and H. T. Davis, *Mesoscale Phenomena in Fluid Systems*, American Chemical Society, 2003, pp. 313-326.

30 11 M. Vasudevan, A. Shen, B. Khomami and R. Sureshkumar, *Journal of Rheology*, 2008, **52**, 527-550.

12 N. Dubash, J. Cardiel, P. Cheung and A. Q. Shen, *Soft Matter*, 2011, **7**, 876-879.

13 J. Yang, *Current opinion in colloid & interface science*, 2002, **7**, 276-281.

35 14 R. Cressely and V. Hartmann, *The European Physical Journal B-Condensed Matter and Complex Systems*, 1998, **6**, 57-62.

15 V. P. Torchilin, *Pharmaceutical research*, 2007, **24**, 1-16.

16 T. H. Ito, P. C. Miranda, N. H. Morgon, G. Heerdt, C. A. Dreiss and E. Sabadini, *Langmuir*, 2014, **30**, 11535-11542

40

17 M.A. Fardin and S. Lerouge, *Soft Matter*, 2014, **10**, 8789-8799.

18 M. Cates, *Macromolecules*, 1987, **20**, 2289-2296.

19 M. E. Cates and S. M. Fielding, *Advances in Physics*, 2006, **55**, 799-879.

45

20 J.F. Berret, *Molecular gels*, Springer, 2006, pp. 667-720.

21 R. L. Moorcroft and S. M. Fielding, *Physical review letters*, 2013, **110**, 086001-5.

22 S. Caserta, M. Simeone and S. Guido, *Physical review letters*, 2008, **100**, 137801-137804.

50

23 T. Clausen, P. Vinson, J. Minter, H. Davis, Y. Talmon and W. Miller, *The Journal of Physical Chemistry*, 1992, **96**, 474-484.

24 E. Cappelaere, J. Berret, J. Decruppe, R. Cressely and P. Lindner, *Physical Review E*, 1997, **56**, 1869-1878.

55 25 U. Olsson, O. Soederman and P. Guering, *The Journal of Physical Chemistry*, 1986, **90**, 5223-5232.

26 N. C. Das, H. Cao, H. Kaiser, G. T. Warren, J. R. Gladden and P. E. Sokol, *Langmuir*, 2012, **28**, 11962-11968.

27 G. Tarabella, G. Nanda, M. Villani, N. Coppedè, R. Mosca, G.

60 G. Malliaras, C. Santato, S. Iannotta and F. Cicoira, *Chem. Sci.*, 2012, **3**, 3432-3435.

28 G. Tarabella, A. G. Balducci, N. Coppedè, S. Marasso, P. D'Angelo, S. Barbieri, M. Cocuzza, P. Colombo, F. Sonvico and R. Mosca, *Biochimica et Biophysica Acta*, 2013, 4374.

65 29 D. A. Bernards and G. G. Malliaras, *Advanced Functional Materials*, 2007, **17**, 3538-3544.

30 D. Nilsson, M. Chen, T. Kugler, T. Remonen, M. Armgarth and M. Berggren, *Advanced Materials*, 2002, **14**, 51-54.

31 H. Rehage and H. Hoffmann, *Molecular Physics*, 1991, **74**, 933-973.

70

32 F. Kern, R. Zana and S. Candau, *Langmuir*, 1991, **7**, 1344-1351.

33 T. Shikata, H. Hirata and T. Kotaka, *Langmuir*, 1988, **4**, 354-359.

75 34 F. Kern, P. Lemarechal, S. Candau and M. Cates, *Langmuir*, 1992, **8**, 437-440.

35 G. Porte, J. Appell and Y. Poggi, *The Journal of Physical Chemistry*, 1980, **84**, 3105-3110.

36 S. Amin, T. W. Kermis, R. M. van Zanten, S. J. Dees and J. H.

80 van Zanten, *Langmuir*, 2001, **17**, 8055-8061.

37 A. Koike, T. Yamamura and N. Nemoto, *Colloid and Polymer Science*, 1994, **272**, 955-961.

38 W. Zhang, G. Li, J. Mu, Q. Shen, L. Zheng, H. Liang and C. Wu, *Chinese Science Bulletin*, 2000, **45**, 1854-1857.

85 39 V. Aswal, P. Goyal and P. Thiyagarajan, *The Journal of Physical Chemistry B*, 1998, **102**, 2469-2473.

40 C. W. Macosko and J. Mewis, *Suspension Rheology*, VCH, 1994.

41 J. D. Ferry, *Viscoelastic properties of polymers*, John Wiley & Sons, 1980.

90

42 G. Tarabella, C. Santato, S. Y. Yang, S. Iannotta, G. G. Malliaras and F. Cicoira, *Applied Physics Letters*, 2010, **97**, 1233041-3.

43 G. Tarabella, A. Pezzella, A. Romeo, P. D'Angelo, N.

95 Coppedè, M. Calicchio, M. d'Ischia, R. Mosca and S. Iannotta, *Journal of Materials Chemistry B*, 2013, **1**, 3843-3849.

44 Z.T. Zhu, J. T. Mabeck, C. Zhu, N. C. Cady, C. A. Batt and G. G. Malliaras, *Chem. Commun.*, 2004, 1556-1557.

45 P. Lin, F. Yan and H. L. Chan, *ACS applied materials & interfaces*, 2010, **2**, 1637-1641.

100